Antilock braking control system for electric vehicles

Chun-Liang Lin, Meng-Yao Yang, En-Ping Chen, Yu-Chan Chen, Wen-Cheng Yu

Department of Electrical Engineering, National Chung Hsing University, Taichung 402, Taiwan
E-mail: chunlin@dragon.nchu.edu.tw

Published in *The Journal of Engineering*; Received on 19th September 2017; Accepted on 17th November 2017

Abstract: In recent years, brushless DC motors (BLDCMs) have replaced brushed DC motors in the design of electric scooters (ESs). This study proposes a new antilock braking system (ABS) based on a slip ratio estimator for ES utilising the braking force generated by the BLDCM when electrical energy is released to the virtual load, yielding an effect analogous to the ABS control in gas-powered vehicles. Compared with mechanical ABS, the proposed design possesses the advantage of rapid torque responses because no mechanical parts needed. Current control design is used to adjust the braking torque, and the sliding-mode control strategy is adopted to regulate the slip ratio to attain the optimal road adhesion during emergency braking. A variety of experiments are conducted for functional and performance verification.

1 Introduction

Vehicle braking under critical conditions such as when wet or slippery road surfaces are encountered or when the driver commits a mistake, usually results in the wheels of the vehicle locking, making the vehicle out of control. Therefore, preventing wheel locking during emergency braking is critical to a safe driving experience, and the antilock braking system (ABS) has thus become standard equipment in modern gasoline-powered vehicles. Various design approaches can be used to improve the performance of ABS, such as sliding-mode control [1, 2], fuzzy logic control [3, 4], adaptive control [5], genetic neural control [6], and the Kalman filter [7]. A non-mechanical ABS controller for electric scooters (ESs) based on regenerative, kinetic, and short-circuit braking mechanisms with a boundary-layer speed control was proposed by our research team [8], with two patents granted [9, 10]. The approach involves using the ES's approximated speed to calculate the value of the slip ratio. However, the research was limited to simulations, and no real-world implementation was attempted.

Here, ABS design for ESs that has an alternate short-circuit braking function is developed; this design is based on our patented concept claimed in [11]. For the braking mechanism, a brushless DC motor (BLDCM) is directly connected to the ground to provide the largest energy dissipation in an intermittent manner with an extremely short duty cycle with the duty cycle controlled via a sliding-mode controller. The sliding-mode control, which considers the non-linear time-varying dynamics of the ES's slip ratio, is used for realising the ABS function.

We introduce a slip ratio estimator (SRE) that requires no vehicle speed measurement, unlike the conventional approach used for gasoline-powered vehicles. A sliding-mode controller is proposed for regulating the slip ratio to reach the ideal value for road adhesion. Various experiments were conducted to demonstrate the effectiveness of the proposed design.

2 System modelling

2.1 Dynamics for electric scooter

A rear-wheel electric drive equipped with a BLDCM propels the rear wheel with a fixed transmission ratio. The dynamics of the BLDCM are simply described as

$$J_{\mathrm{m}}\frac{\mathrm{d}\omega_{\mathrm{m}}}{\mathrm{d}t} = T_{\mathrm{m}} - B_{\mathrm{m}}\omega_{\mathrm{m}} - T_{\mathrm{L}}, \tag{1}$$

$$T_m = -K_m i_e, \tag{2}$$

where T_{m} is the driving torque of the driving motor, ω_{m} is the angular speed of the motor, J_{m} is the inertia of the motor, B_{m} is the damping coefficient, K_{m} is the torque coefficient, i_e is the phase current, and T_L denotes the torque due to the payload.

Fig. 1 shows the torque balance on the rear wheel, and the dynamic equation is expressed as

$$J_{\mathrm{w}}\dot{\omega}_{\mathrm{w}} = T_{\mathrm{w}} + T_{\mathrm{b}} - B_{\mathrm{w}}\omega_{\mathrm{w}} - rF, \tag{3}$$

$$M\dot{V} = F, \tag{4}$$

$$V_{\mathrm{w}} = \omega_{\mathrm{w}} r, \tag{5}$$

where J_{w} is the inertia of the wheel, T_{w} is the generated driving torque, T_{b} is the braking torque, B_{w} is the damping coefficient of the wheel, ω_{w} is the angular speed of the wheel, r is the radius of the rear wheel, F is the friction force, M is the total mass of the ES, V is the velocity of the ES, and $V_{\mathrm{w}} = \omega_{\mathrm{w}} r$ is the tangent velocity of the rear wheel. The transmission system, which has a fixed transmission ratio, can be described as

$$\omega_{\mathrm{w}} = n\omega_{\mathrm{m}}, \quad T_{\mathrm{L}} = nT_{\mathrm{w}}, \tag{6}$$

where n is the gear ratio. By substituting (3) and (6) into (1), the equation of motion of the wheel speed can be obtained as

$$J_{\mathrm{eq}}\dot{\omega}_{\mathrm{w}} = nT_{\mathrm{m}} + n^2 T_{\mathrm{b}} - B_{\mathrm{eq}}\omega_{\mathrm{w}} - n^2 rF, \tag{7}$$

where $J_{\mathrm{eq}} = J_{\mathrm{m}} + n^2 J_{\mathrm{w}}$ and $B_{\mathrm{eq}} = B_{\mathrm{m}} + n^2 B_{\mathrm{w}}$. In (4), the friction force is given by

$$F = Mgu(\lambda), \tag{8}$$

where the slip ratio λ is given by

$$\lambda = \frac{V_{\mathrm{w}} - V}{\max(V_{\mathrm{w}}, V)}. \tag{9}$$

Tyre model is based on Pacejka's magic formula tyre model for motorcycles in general [12, 13].

2.2 Alternate short-circuit braking

In the case of a BLDCM with three pairs of stator windings, the back electromotive force (back-EMF) is regarded as the power

doi: 10.1049/joe.2017.0392

source. It is understandable from the phase current loop generated by the back-EMF. When there is no driving current entering the motor stator and the rotor is still running by inertial rotation, it becomes a power generator with the current generated in the opposite direction to the driving current. By Fleming's left-hand rule, the opposite current would cause a retarding force against motor's forward rotation. One can refer to Fig. 2 for the fact.

Consider the current conduction loop shown in Fig. 3; R and L are the inherent resistance and inductance, respectively, and $E_{a,b,c}$ is back-EMF. The alternate short-circuit brake uses the induced current from the motor back-EMF to control the input and output current directions of the three-phase voltage by a full-bridge inverter for generating a virtual loading effect on the BLDCM; the kinetic brake makes the BLDCM connect to a high-power low-resistance resistor for energy dissipation. When the transistors, e.g. S_1 and S_4, are 'ON', the red loop is constructed as the braking current, as shown in Fig. 3. Similarly, transistors S_1 and S_4, S_1 and S_6, S_3 and S_2, and S_3 and S_6 are alternately turned on to implement the alternate short-circuit braking. The electrical energy dissipates in the braking resistor R_b which is variable according to the breaking current needed. Electronic components used as a dummy load R_b can be a low-resistance resistor or an ultra-capacitor.

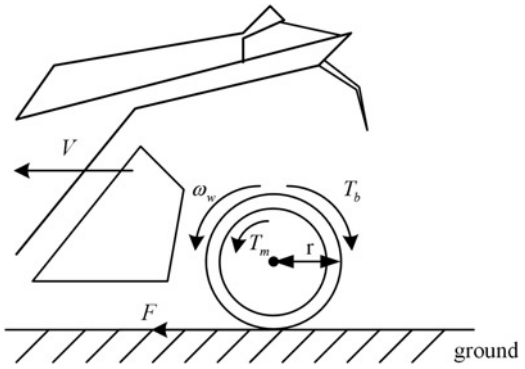

Fig. 1 *Torque balance on the rear wheel*

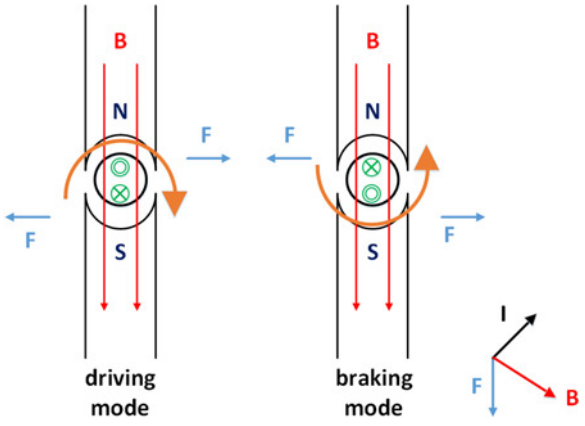

Fig. 2 *Ampère's circuital law describing the force generated under the driving and braking modes*

2.3 Slip ratio estimation

Precise velocity of a vehicle in motion is usually difficult to come by. Here, we formulate an SRE that does not require measuring the vehicle's velocity and acceleration [14].

From (7), the friction force is obtained as

$$F = \frac{nT_{\mathrm{m}} + n^2 T_{\mathrm{b}} - B_{\mathrm{eq}}\omega_{\mathrm{w}} - J_{\mathrm{eq}}\dot{\omega}_{\mathrm{w}}}{n^2 r}. \tag{10}$$

Differentiating (9) with respect to time gives $\dot{\lambda} = (\dot{V}_{\mathrm{w}}/V) - (\dot{V}V_{\mathrm{w}}/V^2)$. Combining (5), (7), and (10) yields

$$\dot{\lambda} = \frac{\dot{\omega}_{\mathrm{w}}}{\omega_{\mathrm{w}}}(1+\lambda) - \left(\frac{nT_{\mathrm{m}} + n^2 T_{\mathrm{b}} - J_{\mathrm{eq}}\dot{\omega}_{\mathrm{w}} - B_{\mathrm{eq}}\omega_{\mathrm{w}}}{n^2 r^2 M \omega_{\mathrm{w}}}\right)(1+\lambda)^2. \tag{11}$$

From the preceding equalities, the unknown variable is observed to be λ. Thus, an SRE can be designed as

$$\dot{\hat{\lambda}} = \frac{\dot{\omega}_{\mathrm{w}}}{\omega_{\mathrm{w}}}(1+\hat{\lambda}) - \left(\frac{nT_{\mathrm{m}} + n^2 T_{\mathrm{b}} - J_{\mathrm{eq}}\dot{\omega}_{\mathrm{w}} - B_{\mathrm{eq}}\omega_{\mathrm{w}}}{n^2 r^2 M \omega_{\mathrm{w}}}\right)(1+\hat{\lambda})^2, \tag{12}$$

where $\hat{\lambda}$ denotes the estimate of the slip ratio. To analyse the convergence of the SRE, the estimation error is defined as $e = \lambda - \hat{\lambda}$. The error dynamics is given by

$$\dot{e} = \left[\frac{\dot{\omega}_{\mathrm{w}}}{\omega_{\mathrm{w}}} - \frac{nT_{\mathrm{m}} + n^2 T_{\mathrm{b}} - J_{\mathrm{eq}}\dot{\omega}_{\mathrm{w}} - B_{\mathrm{eq}}\omega_{\mathrm{w}}}{n^2 r^2 M \omega_{\mathrm{w}}}(2 + \lambda + \hat{\lambda})\right] e. \tag{13}$$

Equivalently

$$\dot{e} = \frac{1}{V_{\mathrm{w}}}\left[\dot{V}_{\mathrm{w}} - \dot{V}(2 + \lambda + \hat{\lambda})\right] e. \tag{14}$$

Clearly, the estimation error e converges to zero if

$$\dot{V}_{\mathrm{w}} < \dot{V}(2 + \lambda + \hat{\lambda}). \tag{15}$$

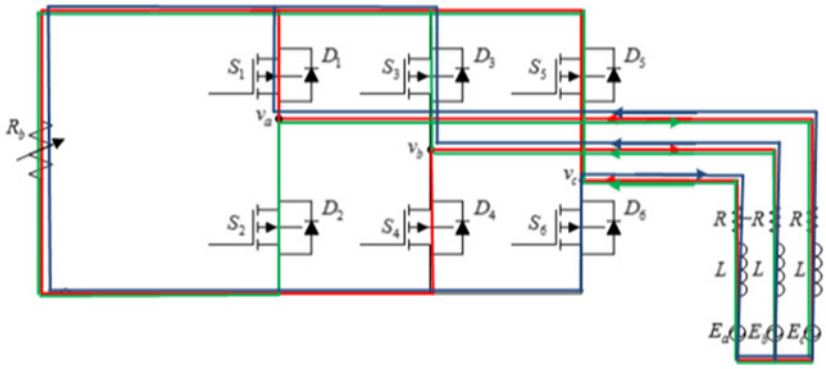

Fig. 3 *Current flow in alternate short-circuit braking mode with power transistors switched on alternately*

doi: 10.1049/joe.2017.0392

Because λ is very small, the inequality is close to $\dot{V}_w < \dot{V}(2 + \hat{\lambda})$. During vehicle braking, because $\dot{V}_w \leq 0$, $\dot{V} \leq 0$, and $\dot{V}_w \leq \dot{V}$ (wheel stops before the vehicle), and because λ is very small, (15) can be satisfied.

3 Control design

Here, a wheel-slip controller is designed to achieve a target slip ratio for a given driving condition. The ABS design utilises the braking force generated from the BLDCM of the rear wheel when electrical energy is released to the dummy load as the braking action occurs. A proportional–integral (PI) current controller is designed to determine the pulse-width modulation (PWM) duty cycle at each sampling instant according to the difference between braking and reference currents. Furthermore, a slip-ratio sliding-mode controller is proposed for calculating the reference current as the reference input to the PI current controller (Fig. 4).

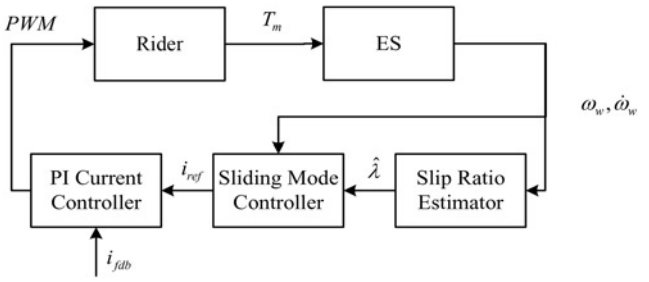

Fig. 4 *Overall braking control scheme*

3.1 Control for slip ratio

Sliding-mode control is an effective method for controlling a nonlinear plant and is a simple approach to overcoming the control problem [1, 2]. Here, a sliding-mode controller is designed to regulate the slip ratio to attain optimal road adhesion. The design procedure for the sliding-mode controller comprises two steps: first, a sliding surface that models the desired tracking performance is defined. Then, a control law for forcing the state trajectories towards the sliding surface is developed. Equation (11) can be rearranged as follows:

$$\dot{\lambda} = f_1(\lambda, t) + b_1(\lambda, t)u_1, \tag{16}$$

where

$$f_1(\lambda, t) = \frac{\dot{\omega}_w}{\omega_w}(1 + \lambda) + \left(\frac{J_{eq}\dot{\omega}_w + B_{eq}\omega_w}{n^2 r^2 M \omega_w}\right)(1 + \lambda)^2,$$

$$b_1(\lambda, t) = \left(\frac{-1}{nr^2 M \omega_w}\right)(1 + \lambda)^2$$

and $u_1 = T_m = -K_T i$.

The sliding surface is selected as $s = c\tilde{\lambda}$, where c is a constant, $\tilde{\lambda} = \lambda - \lambda_{idl}$ with λ_{idl} being the ideal value of λ. Differentiating s with respect to time gives

$$\dot{s} = c\dot{\lambda}. \tag{17}$$

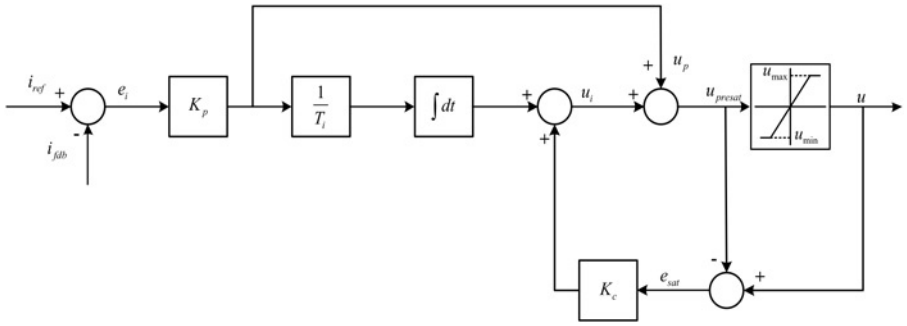

Fig. 5 *PI current control with antiwindup correction*

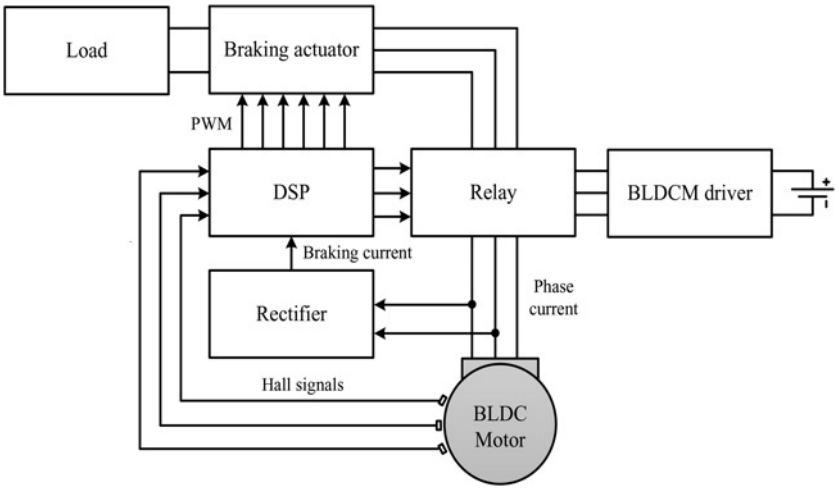

Fig. 6 *Schematic of the control system*

Table 1 Parameters for experimental verification

Item	Numerical value
total mass	120 kg
wheel radius	0.2 m
battery voltage	48 V (12 V×4)
armature inductance	0.0023 H
armature resistance	1.1 Ω
motor inertia	0.000568 kg m^2
motor torque constant	0.18 Nm/A
back-EMF constant	0.18 V/rad/s

By equating (17) to zero, the equivalent control can be obtained as

$$u_{eq} = \frac{nr^2 M\dot{\omega}_w}{1+\lambda} + \frac{J_{eq}\dot{\omega}_w + B_{eq}\omega_w}{n}. \tag{18}$$

To satisfy the sliding condition, the total control law is set to be

$$u_1 = u_{eq} + \beta \mathrm{sgn}(s) \tag{19}$$

with β being a constant.

In real-world applications, the system parameters are frequently uncertain. Considering the major system uncertainty, the control

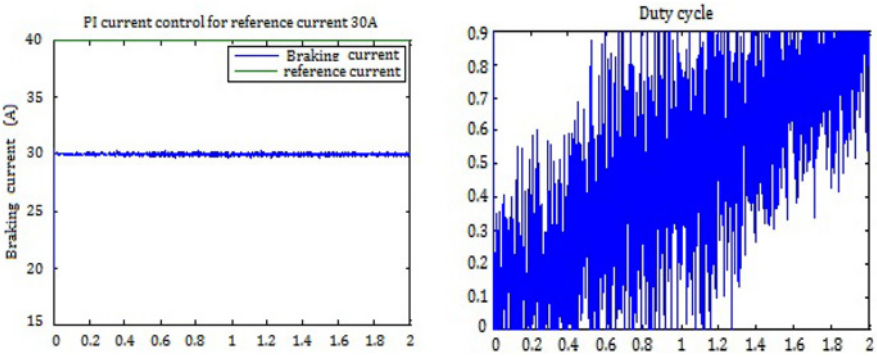

Fig. 7 *PI current control: braking current (left), changes in duty cycle (right)*

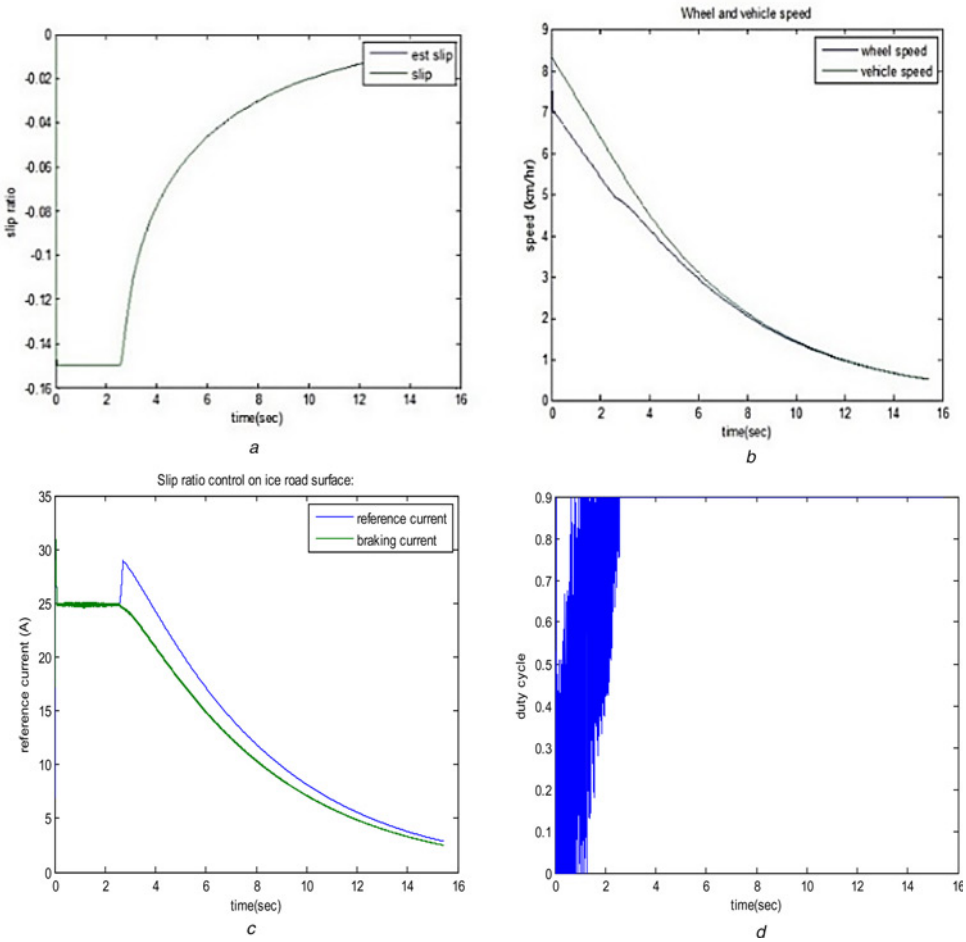

Fig. 8 *Slip ratio control on icy road*
a Slip ratio and estimated slip ratio
b Wheel speed and vehicle speed
c Braking current and reference current
d PWM duty cycle

doi: 10.1049/joe.2017.0392

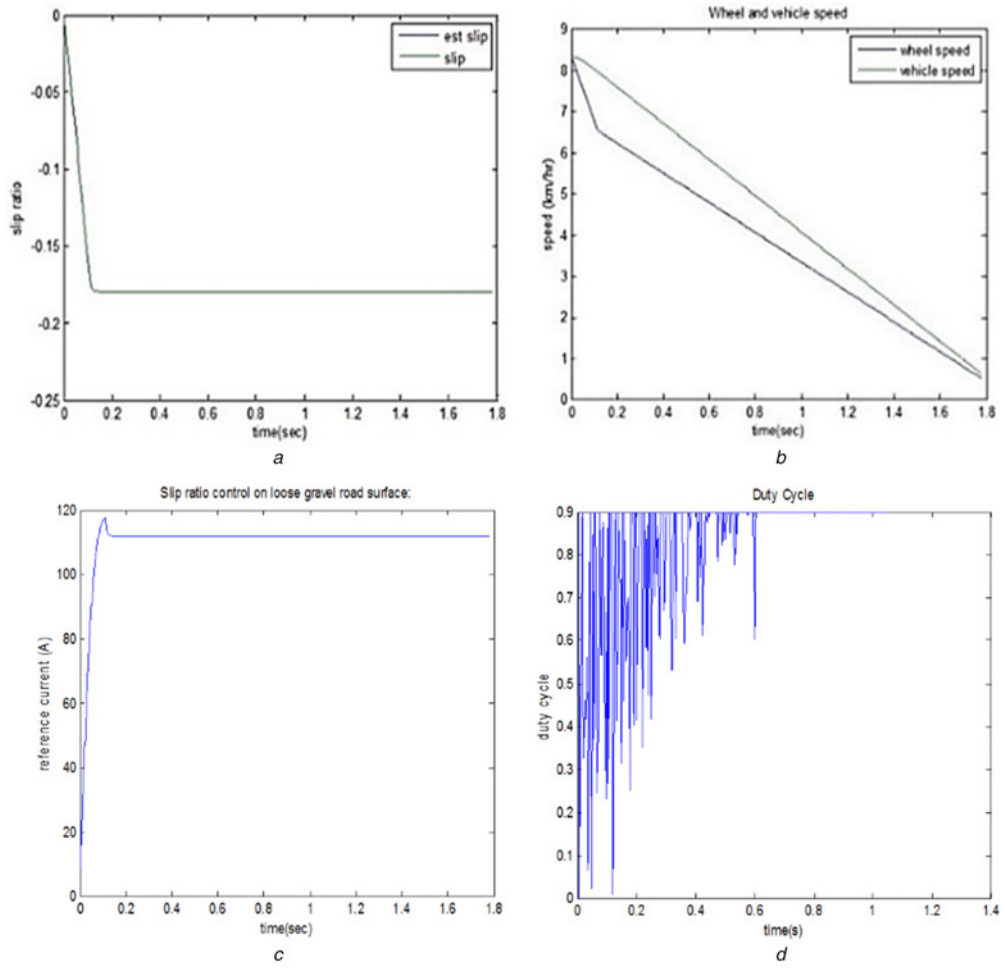

Fig. 9 *Slip ratio under sliding-mode control on the loose gravel road*
a Slip ratio and estimated slip ratio
b Wheel speed and vehicle speed
c Reference current
d PWM duty cycle

input should be chosen as

$$u_1 = \frac{1}{b_0(\lambda, t)}(u_2 - f_0(\lambda, t)), \tag{20}$$

where u_2 is to be determined, and

$$f_0(\lambda, t) = \frac{\dot{\omega}_w}{\omega_w}(1+\lambda) + \left(\frac{J_{eq}\dot{\omega}_w + B_{eq}\omega_w}{n^2 r^2 M_0 \omega_w}\right)(1+\lambda)^2, \tag{21}$$

and

$$b_0(\lambda, t) = \left(\frac{-1}{nr^2 M_0 \omega_w}\right)(1+\lambda)^2, \tag{22}$$

where $M_0 = 0.5(M_{max} + M_{min})$, with M, M_{min}, and M_{max} denoting the nominal, lower, and upper bounds, respectively. The system equation can be expressed as

$$\dot{\lambda} = d + bu_2, \tag{23}$$

where $b = M_0 M^{-1}$, $d = (\dot{\omega}_w/\omega_w)(1+\lambda)\Delta_n M$, with $\Delta_n M = (M - M_0)/M$ and $|\Delta_n M| \le \varepsilon_m$.

Suppose $d_{min} < d < d_{max}$, where $d_{min} = (\dot{\omega}_w/\omega_w)(1+\lambda_{min})\varepsilon_m$ and $d_{max} = (\dot{\omega}_w/\omega_w)(1+\lambda_{max})\varepsilon_m$ specify the lower and upper bounds, respectively. The estimate of d is given by $\hat{d} = (d_{min} + d_{max})/2$. Then, $|\hat{d} - d| \le D$, where $D = (d_{max} - d_{min})/2$. The input gain is bounded by $0 < b_{min} \le b \le b_{max}$, where the geometric mean of b_{min} and b_{max} can be defined as the estimate of b as $\hat{b} = \sqrt{b_{min} b_{max}}$. From the preceding equations, we obtain $\varphi^{-1} \le b\hat{b}^{-1} \le \varphi$, where $\varphi = \sqrt{b_{max} b_{min}^{-1}}$. The control law u_2 in (20) is proposed as

$$u_2 = \hat{b}^{-1}(-\hat{d} - k_a \mathrm{sgn}(s)). \tag{24}$$

To satisfy the sliding condition, let us consider

$$\begin{aligned} s\dot{s} &= s\left\{d + b\hat{b}^{-1}[-\hat{d} - k_a \mathrm{sgn}(s)]\right\} \\ &\le |s|\left(|d - \hat{d}| + |\hat{d}|\left|1 - b\hat{b}^{-1}\right| - b\hat{b}^{-1}k_a\right). \end{aligned} \tag{25}$$

We set $\eta + |d - \hat{d}| + |\hat{d}|\left|1 - b\hat{b}^{-1}\right| \le b\hat{b}^{-1}k_a$, where η is a positive constant that determines the convergence rate of $\tilde{\lambda}$ reaching the sliding surface. Then, the sliding condition $s\dot{s} \le -\eta|s|$ is satisfied. Considering

$$\begin{aligned} &\eta + |d - \hat{d}| + |\hat{d}|\left|1 - b\hat{b}^{-1}\right| - b\hat{b}^{-1}k_a \\ &\le \eta + D + |\hat{d}||\varphi - 1| - \varphi^{-1}k_a \le 0, \end{aligned} \tag{26}$$

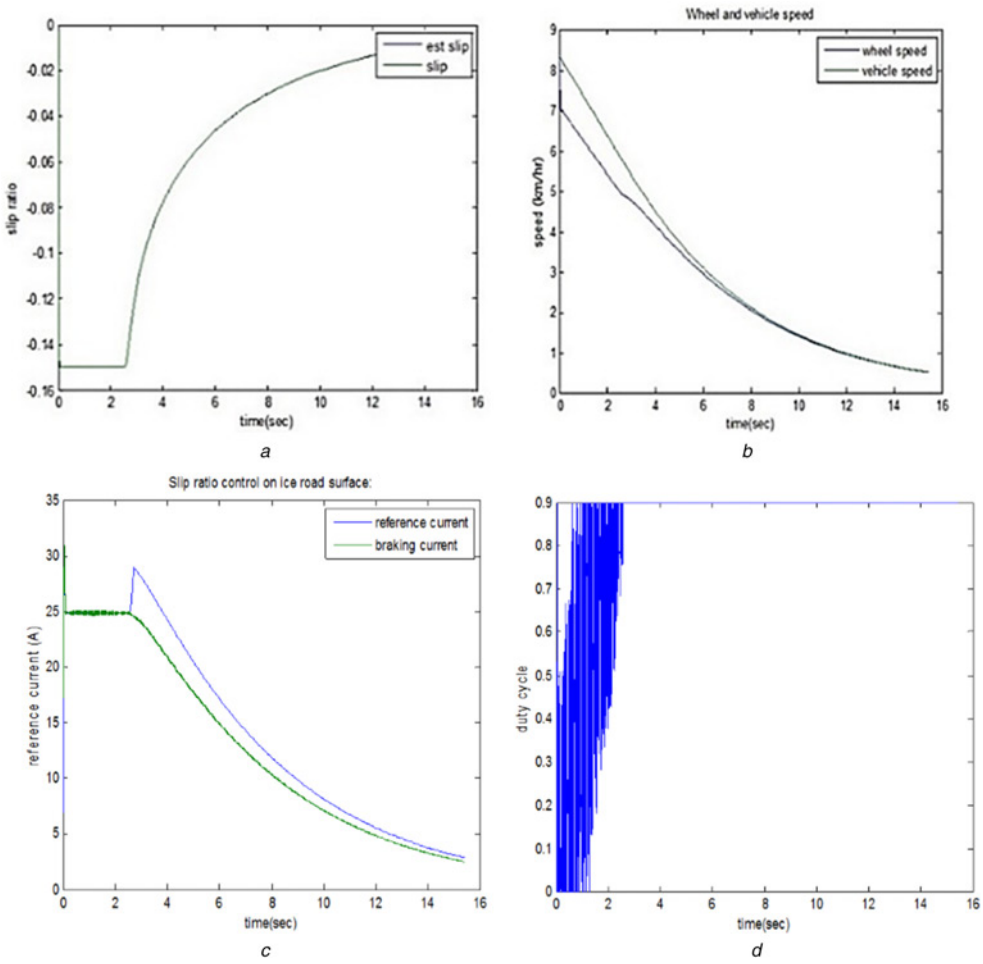

Fig. 10 *Slip ratio control on icy road*
a Slip ratio and estimated slip ratio
b Wheel speed and vehicle speed
c Braking current and reference current
d PWM duty cycle

the gain k_a in (24) becomes

$$k_a = \varphi(\eta + D + |\hat{d}||\varphi - 1|). \tag{27}$$

This can be specified based on the specifications given above.

3.2 Current control

PI current controller is designed to track the reference current computed by the slip-ratio sliding-mode controller. The input to the PI current controller is $e_i = i_{\text{ref}} - i_{\text{fdb}}$, where e_i is the difference between the reference and feedback currents, i_{ref} is the reference input, and i_{fdb} is the feedback braking current. The PI current controller with antiwindup before saturation is given by

$$u_{\text{presat}}(t) = u_{\text{p}}(t) + u_{\text{i}}(t), \tag{28}$$

where the proportional term $u_{\text{p}}(t) = K_{\text{p}} e_i(t)$ and the integral term $u_{\text{i}}(t) = (K_{\text{p}}/T_{\text{i}}) \int e_i(\varsigma)\mathrm{d}\varsigma + K_{\text{c}}(u(t) - u_{\text{presat}}(t))$, with $u_{\text{presat}}(t)$ being the output before saturation, $u(t)$ the output of the PI–derivative controller, K_{p} is the proportional gain, T_{i} is the integral time, and K_{c} is the integral correction gain. A block diagram of the PI current controller with antiwindup correction is shown in Fig. 5.

Digital signal processor (DSP) is used to determine which transistors should be ON according to the Hall signals that are used to determine the rotational speed of the motor. On the basis of the feedback commands received, the DSP calculates the duty cycle to adjust the braking force and thus regulate the slip ratio to attain the ideal value for road surface adhesion.

4 Experimental verification

4.1 Experimental setting

Block diagram of the designed system is presented in Fig. 6. The parameters used for simulating the control of the braking current are listed in Table 1.

The ES's initial speed was set to be 30 km/h. The PI current controller is designed to track the reference current determined by the slip-ratio sliding-mode controller as described in Section 5. The kinetic energy, however, may decrease during the braking process. The duty cycle (i.e. the percentage of time for which current flows over the sampling period) for braking current regulation was increased to maintain the optimal slip ratio. Fig. 7 shows the PI current control command with a reference current of 40 A for the braking mode.

4.2 Simulation results

Sliding-mode controller is designed to determine the appropriate braking force for maintaining the ideal slip ratio. Braking was simulated on three road surfaces: dry road, loose gravel road, and icy road. The ideal slip ratio values of the three road surfaces are 0.2, 0.18, and 0.15, respectively. Suppose that the mass of the ES

doi: 10.1049/joe.2017.0392

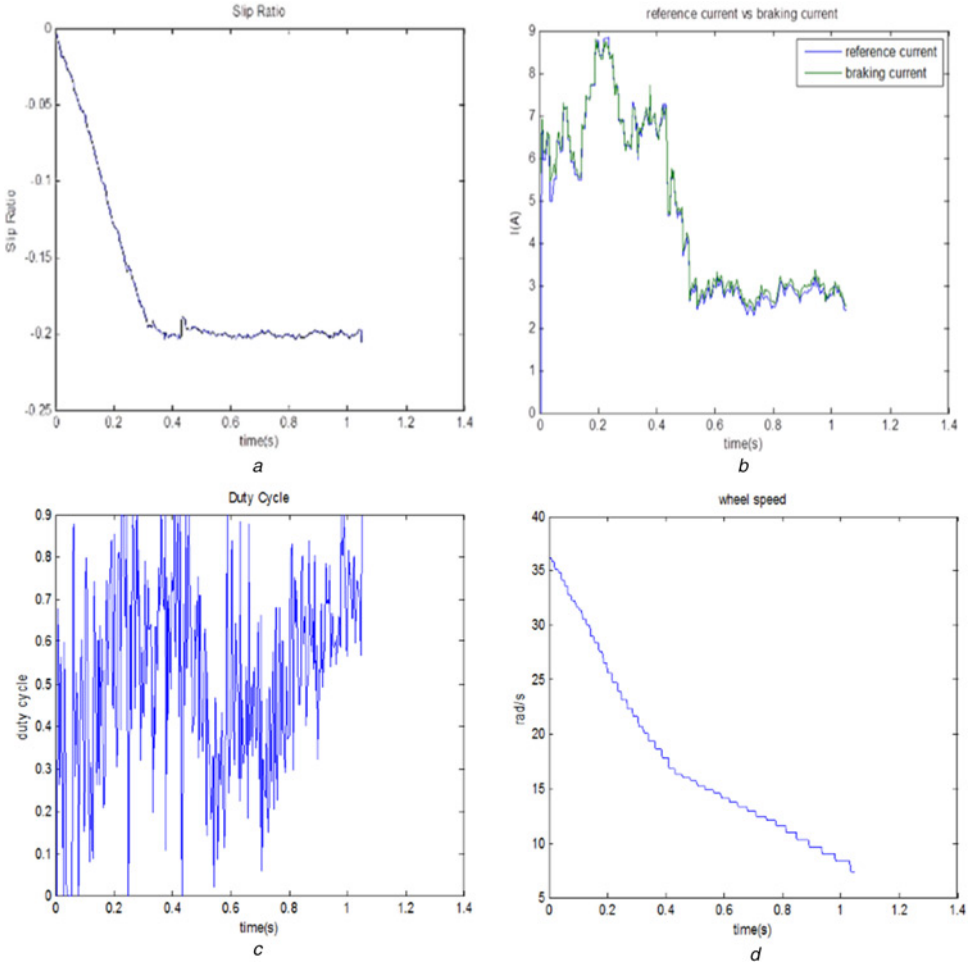

Fig. 11 *Experimental results of the SRE under sliding-mode control*
a Estimated slip ratio
b Braking and reference currents
c PWM duty cycle
d Wheel angular speed

with the total weight varying within the range $M_{\min}(=150\,\text{kg}) \le M \le M_{\max}(=240\,\text{kg})$. The non-linear time-varying term d varies within the range $d_{\min}(=-0.1428) \le d \le d_{\max}(=0.1142)$. This gives $\hat{d}=0.5(d_{\min}+d_{\max})$, and $\hat{d}=-0.0143$.

Accordingly, the estimation error of d is bounded by $|d-\hat{d}| \le D(=0.1285)$. The upper and lower bounds of the input gain are obtained as $b_{\min}(=0.75) \le b \le b_{\max}(=1.2)$.

Thus, its geometric mean is $\hat{b}=\sqrt{b_{\min}b_{\max}}=0.9487$, and therefore, $\varphi^{-1}(=0.7906) \le b^{-1}\hat{b} \le \varphi(=1.2649)$.

Figs. 8–10 show the simulated results for slip ratio control on dry, loose gravel, and icy road surfaces, respectively. The slip ratio is kept close to the ideal value on the icy road surface, and the braking current follows the reference current for the first 2.8 s. Because the wheel speed drops thereafter, the back-EMF is not sufficient to support the braking current. The ES speed decreases accordingly, and the ES steering cannot be controlled well. The braking current does not follow the reference current after 3.8 s, and the ABS is inactive because of the decrease in kinetic energy. This shows that the present approach performs satisfactorily on the dry and gravel surfaces but not on the icy surface.

4.3 *Real-world experimental results*

For the friction coefficient between the tyre and dry road surface, the appropriate slip ratio for optimal road adhesion is nearly −0.2. When the proposed design was used, the actual slip ratio converged gradually to the preset value of −0.2 during braking, as shown in Fig. 11*a*. The braking current followed the reference command because of the sliding-mode control, as illustrated in Fig. 11*b*. Fig. 11*c* shows the duty cycle for braking current regulation, which was adjusted by the PI current controller. Fig. 11*d* shows the deceleration of the wheel angular speed after braking.

Please visit the website [15] *for experiments we have conducted in the lab and real-world condition.* In the first video, description of the system hardware and fundamental experimental tests in a platform installing a single driving wheel are presented. In the second video, we have compared the braking performance of the traditional mechanical brake (under the situation of fully locked brake) and the proposed ABS design on the road with smooth and rough surfaces. Fig. 12 and Table 2 present performance of our proposed design. It can be seen from the video clip, how the proposed design avoiding the rear wheel from siding during emergency braking.

5 Conclusions

This paper proposes ABS control design for ESs based on an SRE, which utilises braking torque generated by BLDCM when regenerated energy is released to a virtual load. Mathematical models of the BLDCM and SRE were formulated for theoretical analysis of the braking behaviour. Braking performance of the ES was experimentally validated; the electrical ABS operates well because of the faster torque response of the BLDCM when the ES moves on roads with different surface adhesion. Extensive

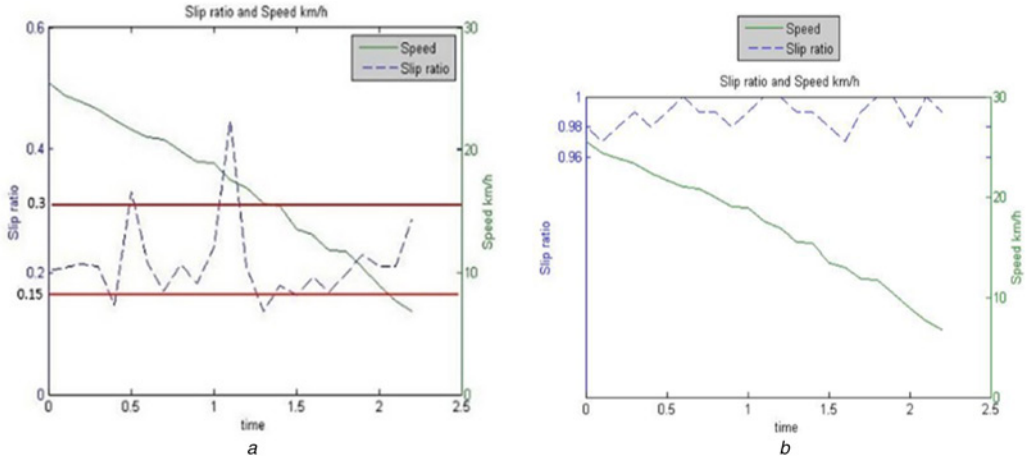

Fig. 12 *Comparison of the slip ratio between the proposed brake (left) and the mechanical brake (right)*

Table 2 Experimental results for the proposed brake and mechanical brake

Brake item	Brake time at the rough road surface, s	Brake time at the smooth road surface, s	State of wheel	Distances, m
mechanical	1.9	2.3	locked	7.5
electromagnetic	2.02	2.1	ABS	7.4

real-world tests have verified the proposed design and its effectiveness during emergency braking.

6 Acknowledgments

This research was sponsored by Ministry of Science and Technology, Taiwan under the grant MOST 104-2221-E-005-093-MY2.

7 References

[1] Kayacan E., Oniz Y., Kaynak O.: 'A grey system modeling approach for sliding-mode control of antilock braking system', *IEEE Trans. Ind. Electron.*, 2009, **56**, pp. 3244–3252

[2] Peng Q., Liu J., Huang Z., *ET AL.*: 'Sliding model control based on estimation of optimal slip ratio for railway wheel slide protection using extremum seeking'. Proc. IEEE Energy Conversion Congress and Exposition, 2016, pp. 1–6

[3] Precup R.E., Preitl S., Radac M.B., *ET AL.*: 'Experiment-based teaching in advanced control engineering', *IEEE Trans. Educ.*, 2011, **54**, pp. 345–355

[4] Dai C.L., Xu L.J.: 'The simulation research of automobile ABS system based on fuzzy theory'. Proc. Int. Conf. Intelligent Transportation, Big Data and Smart City, 2015, pp. 922–926

[5] Su S.F., Chang J.C., Chen S.S.: 'The study on direct adaptive fuzzy controllers', *Int. J. Fuzzy Syst.*, 2006, **8**, pp. 150–159

[6] Lee Y.G., Zak S.H.: 'Designing a genetic neural fuzzy antilock-brake-system controller', *IEEE Trans. Evol. Comput.*, 2002, **6**, pp. 198–211

[7] Zhang Y., Zhao H., Yuan L., *ET AL.*: 'Slip ratio estimation for electric vehicle with in-wheel motors based on EKF without detection of vehicle velocity'. Proc. Chinese Control and Decision Conf., 2016, pp. 4427–4432

[8] Lin W.C., Lin C.L., Hsu P.M., *ET AL.*: 'Realization of anti-lock braking strategy for electric scooters', *IEEE Trans. Ind. Electron.*, 2014, **61**, pp. 2826–2833

[9] Lin C.L., Lin W.C.: 'Two wheel-drive electric motorcycle having a braking controller for generating a breaking effect similar to the anti-lock braking system'. Taiwan Patent no. I 370078, Taiwan, valid 2012–2030

[10] Lin C.L., Huang C.D.: 'Electric motorcycle having a braking effect similar to the anti-lock braking system'. Taiwan Patent no. I 384733, valid 2013–2029

[11] Lin C.L., Lin W.C.: 'System of braking force adjusting scheme for electronic anti-locking braking system'. Taiwan Patent no. I 472451, valid 2015–2032

[12] Pacejka H.B., Besselink I.J.M.: 'Magic formula tyre model with transient properties', *Veh. Syst. Dyn.*, 1997, **27**, pp. 234–249

[13] de Vries E.J.H., Pacejka H.B.: 'Motorcycle tyre measurements and models', *Veh. Syst. Dyn.*, 1998, **29**, pp. 280–2982

[14] Suzuki T., Fujimoto H.: 'Slip ratio estimation and regenerative braking control without detection of vehicle velocity and acceleration for electric vehicle at urgent brake-turning'. Proc. Int. Workshop on Advanced Motion Control, 2010, pp. 273–278

[15] https://sites.google.com/site/bccl606/research/videos